Egyptian Journal of Radiology and Nuclear Medicine

RESEARCH

Open Access

Diffusion tensor imaging in characterization of cervical lymphadenopathy

Zainab A. Ramadan[1*] and Ahmed Abdel Razek[1]

Abstract

Background It is important to differentiate cervical lymph nodes. So, this study aims to assess the ability of diffusion tensor imaging (DTI) in differentiating cervical lymphadenopathy (LNs).

Materials and methods This retrospective study was done upon 100 patients with cervical LNs who had DTI over a year period. The fractional anisotropy (FA) and the mean diffusivity (MD) values of LNs were measured.

Results This study was done upon 100 patients (the mean age 45 ± 2 years (standard deviation [SD]), 63 men). The mean MD and FA of the malignant LNs ($0.83 \pm 0.14 \times 10^{-3}$ mm^2/s, 0.26 ± 0.07) were significantly different; ($P = 0.001$) than those of benign LNs ($1.32 \pm 0.33 \times 10^{-3}$ mm^2/s, 0.22 ± 0.09). MD of 0.94×10^{-3} mm^2/s and FA of 0.21 were used to discriminate malignant and benign LNs, AUC 0.892 and 0.758, and 84% and 71% accuracy, respectively. Combined parameters revealed AUC of 0.914 and 81%. The mean MD and FA of the metastatic LNs ($0.86 \pm 0.12 \times 10^{-3}$ mm^2/s, 0.25 ± 0.07) were statistically different; ($P = 0.001$, 0.03) than those of lymphomatous nodes ($0.66 \pm 0.13 \times 10^{-3}$ mm^2/s, 0.28 ± 0.02). The AUC of the MD and FA used to distinguish metastatic from lymphomatous nodes was 0.82, 0.711, (0.71×10^{-3} mm^2/s, 0.27) cutoff values, and 95.3%, 73.4% accuracy, respectively. Combined parameters revealed 0.824 AUC, 95.3% accuracy, 98.2% sensitivity, and 75% specificity. There was a significant statistical difference in MD between well-moderately ($P = 0.001$) versus poorly differentiated metastatic LNs and stages I and II ($P = 0.018$) versus stages III and IV of metastatic cervical LNs.

Conclusions Combining FA and MD is a promising technique that can play a major role in distinguishing different categories of cervical LNs.

Keywords Tensor, Diffusion, MRI, Metastatic, Cervical, Malignant LNs

Background

Assessment of cervical LNs is one of the most challenging issues for the radiologist. When a LN is detected, the radiologist has to delineate whether it is of benign or malignant nature [1, 2]. Ultrasound together with fine-needle aspiration biopsy (FNAC) was widely used, yet it is a relatively invasive, operator-dependent modality that has a tendency to false-positive and -negative results [3, 4]. Differentiation between different types of cervical LNs is difficult with conventional computed tomography (CT) and magnetic resonance (MR) [5–7].

Advanced MR imaging modalities as post-contrast, dynamic MRI, MR spectroscopy, as well as arterial spin labeling are used to add in characterization, but unfortunately, their value is relatively limited [7–11]. Advanced CT techniques as CT perfusion and dual-energy CT carry the risks of radiation exposure and contrast administration, and PET-CT is costly, not widely available and of low spatial resolution [12, 13].

Pathological diagnosis is the ideal modality for the evaluation of the nature of cervical LNs, but it may be inconclusive, or of inadequate samples. Fine-needle aspiration biopsy is immensely used, yet it is a relatively invasive,

*Correspondence:
Zainab A. Ramadan
zainabahmed87@mans.edu.eg
[1] Department of Diagnostic and Interventional Radiology, Faculty of Medicine, Mansoura University, Elgomhoria Street, Mansoura 35516, Egypt

operator-dependent modality with a relatively high rate of inaccurate results [14].

Diffusion-weighted imaging (DWI) is based mainly on the Brownian mobility of water protons in different tissues, which is controlled by the cellular and extra-cellular structures of these tissues, so it has the ability to discriminate different tissues compartments at a cellular level [15–20]. Variable studies reported the benefit of DWI in distinguishing between subtypes of LNs in different parts of the body [21–25] and in cervical LNs that might be associated with artifacts in the neck and head region [26–30].

Diffusion tensor imaging (DTI) utilizes the benefit of water flow and diffusivity within tissue within the three primary directions. This motion is relatively decreased in the plane perpendicular to the cellular membranes. The most popular parameters of DTI are FA and MD. The MD delineates the mobility and flow rate of the water molecules as the cellularity within the lesion is the major goal of pathological classification of lesions with DTI. The relation between the degree of cellularity and MD value is negative. The FA delineates the orientation of microstructures and nearby different tissues [31–33].

Diffusion tensor evaluates the water protons motion in tissues as well as their spatiality. The protons that move only in a single direction are called anisotropic and their FA equals 1. The protons that move in any direction, in the same manner, are called isotropic and their FA equals 0. A highly cellular tumor is anticipated to have both; low diffusivity and anisotropy as it has limited extra-cellular space, whereas a low cellular tumor that is mostly benign might have relatively higher diffusivity and high anisotropy [34–36]. Few studies discuss the reliability of DTI in the valuation of neck and head malignancies, distinguishing recurrent neck and head cancer from post-treatment changes, and characterization of salivary gland tumors [36–40].

Aim of the work is to assess the role of DTI in characterization of cervical LNs.

Materials and methods

Patients

This research was approved by the institutional review board, and the patients' informed consent was waived because this was a retrospective study. This retrospective study was done on 105 patients from 2019 to 2020 with cervical LNs. The criteria of inclusion were patients with cervical LNs referred for MR suspected to be malignant. Five patients were excluded from this study because of motion artifacts. So, the included patients in the study were 100 patients (63 males and 37 females, with their ages ranging from 18 to 72 years, the mean age 45 ± 2 years). The definitive diagnosis was obtained by surgical biopsy and core biopsy that done 7–14 days after MRI. All patients had routine imaging as well as DTI of the neck and head.

Methods

MR imaging

Magnetic resonance images were obtained on a 1.5-T scanner (Ingenia Philips, Philips Medical Systems, Best Netherlands) with a self-shielding gradient set (30-mTm maximum gradient strength, 120 T/m/s rate) and a 16-channel neurovascular coil. All the patients had T1-weighted image (TR/TE = 800/15 ms) and T2-fast spin-echo weighted image (TR/TE = 6000/80 ms) with these parameters; thickness of section 5 mm, gap between slices 1.5 mm, a field-of-view (FOV) 25–30 cm^2, and matrix of acquisition 256 × 224.

Diffusion tensor imaging

Diffusion tensor MR imaging of the neck has been obtained through a single-shot echo-planar sequence (TR/TE 3200/90 ms) together with parallel imaging. Gradients of diffusion had been acquired along 32 axes, *b*-values of 0 and 1000 s/mm^2 were used, matrix = 92 × 88, FOV = 250 × 170 mm^2, and voxel dimensions = 2.43 × 2.54 × 2.5 mm^3. Forty-eight slices have been obtained, with a thickness of 2.5 mm, no gap. The full scan time was about 7–8 min.

Image analysis

Analysis of the images was carried out by one neck and head radiologist with 10 years' experience who was blind to the definitive results. Co-registration of DTI maps with T2 images was performed for correct positioning of the region of interest (ROI). The largest LN that showed homogenous texture in each patient was selected for analysis. The ROI was placed at DTI map-guided with T2-weighted imaging around the inner border of the LN using the electronic cursor (Fig. 1). The size of the ROI varied between 4.4 and 19.6 mm^2 (mean 9.4 mm^2).

Statistical analysis

The statistical analysis of these data was done using the Statistical Package for the Social Sciences version 22 (SPSS Inc., Chicago, Ill, USA). The mean and standard deviation of MD and FA of metastatic, lymphomatous, and benign LNs have been measured. Analysis of these data was done so as to test the significant statistical differences. The Student's t-test has been used for comparison between MD and FA of LNs. *P*-value < / = 0.05 was considered significant. The receiver operating characteristic (ROC) curve was used to detect the cutoff points of MD and FA utilized in differentiating malignant from benign LNs and metastatic from lymphomatous LNs

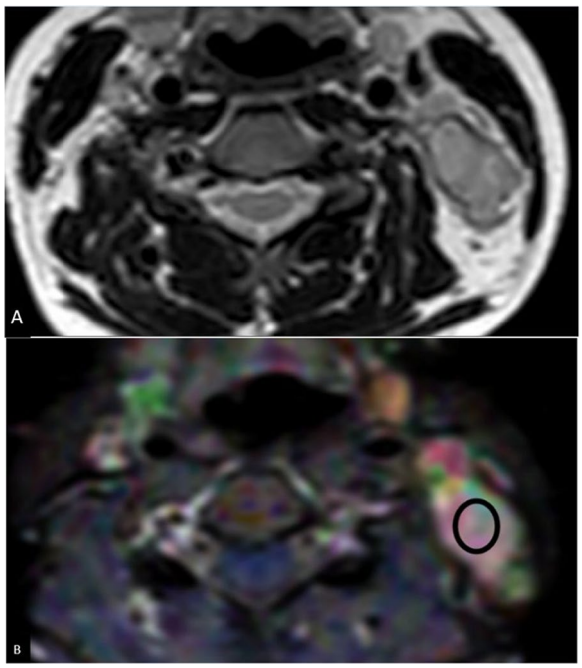

Fig. 1 Region of interest definition of metastatic cervical LNs. **A** Axial T2 image displays enlarged left-sided neck LN. **B** DTI map displays enlarged cervical LN with calculated MD value of $0.91 \times 10^{-3} mm^2/s$ and FA of 0.53

with computation of area under the curve (AUC), accuracy, specificity, and sensitivity.

Results

The causes of LNs pathogenesis were; metastatic ($n=56$), lymphoma ($n=8$), and benign ($n=36$). Metastatic LNs were secondary to squamous cell carcinoma of the mouth; ($n=24$), larynx; ($n=8$), oropharynx; ($n=8$), nasopharynx; ($n=8$), and sino-nasal; ($n=8$). Lymphomatous nodes were non-Hodgkin's lymphoma (NHL); ($n=5$) and Hodgkin's disease (HD); ($n=3$). Benign LNs were reactive ($n=32$) and granulomatous ($n=4$) either sarcoidosis ($n=2$) or tuberculous ($n=2$). Table 1 shows MD and FA of cervical LNs. Table 2 shows the ROC results with cutoff points of MD and FA used in differentiating cervical LNs.

The mean MD of malignant LNs ($0.83 \pm 0.14 \times 10^{-3}$ mm^2/s) was statistically lower than ($P=0.001$) the MD of benign LNs ($1.32 \pm 0.33 \times 10^{-3}$ mm^2/s). The mean FA of malignant cervical LNs (0.26 ± 0.07) was statistically higher than ($P=0.02$) that of benign cervical LNs (0.22 ± 0.09). The cutoff points of MD and FA used to discriminate benign from malignant LNs were 0.94×10^{-3} mm^2/s, 0.21 with AUC equals 0.892, 0.758, accuracy of 84%, 71%, specificity of 88.9%, 50%, and sensitivity of 81.2%, 82.8%, respectively. Combined parameters revealed AUC of 0.914, with accuracy of 81%, specificity of 77.8%, and sensitivity of 92.2% (Fig. 2).

Table 1 Mean, SD, minimum, and maximum of MD ($\times 10^{-3}$ mm^2/s) and FA of malignant, benign, metastatic, lymphomatous, well-moderately, poorly differentiated, and different stages of cervical lymph nodes

	MD	FA
Malignant ($n=64$)	0.83 ± 0.14	0.26 ± 0.07
Benign ($n=36$)	1.32 ± 0.33	0.22 ± 0.09
P value	0.001	0.02
Metastatic ($n=56$)	0.86 ± 0.12	0.25 ± 0.07
Lymphoma ($n=8$)	0.66 ± 0.13	0.28 ± 0.02
P value	0.001	0.03
Well-moderate differentiated ($n=39$)	0.81 ± 0.06	0.26 ± 0.08
Poorly differentiated ($n=17$)	0.96 ± 0.16	0.23 ± 0.04
P value	0.001	0.23
Stages I and II ($n=15$)	0.88 ± 0.13	0.22 ± 0.04
Stages III and IV ($n=41$)	0.80 ± 0.05	0.26 ± 0.08
P value	0.018	0.69

The mean MD of metastatic LNs ($0.86 \pm 0.12 \times 10^{-3}$ mm^2/s) was statistically higher than ($P=0.001$) the lymphoma ($0.66 \pm 0.13 \times 10^{-3}$ mm^2/s). The mean FA of metastatic LNs (0.25 ± 0.07) was statistically lower than ($P=0.03$) lymphomatous nodes (0.28 ± 0.02). On the ROC curve; the MD and FA area under curve used to distinguish metastatic from lymphomatous nodes were 0.82, 0.711 with the cutoff values of 0.71×10^{-3} mm^2/s, 0.27, an accuracy of 95.3%, 73.4%, sensitivity of 98.2%, 76.8%, and specificity of 75%, 50%, respectively. Combined parameters resulted in an AUC of 0.824, with an accuracy of 95.3%, sensitivity 98.2%, and specificity 75% (Fig. 3).

Table 2 Validity of MD ($\times 10^{-3}$ mm^2/s) and FA in characterization of cervical lymph nodes

	AUC	Cutoff	Sensitivity	Specificity	Accuracy
Malignant versus benign					
MD	0.892	0.94	81.2	88.9	84.0
FA	0.758	0.21	82.8	50.0	71.0
Combined	0.914		92.2	77.8	81.0
Metastatic versus lymphoma					
MD	0.820	0.71	98.2	75.0	95.3
FA	0.711	0.27	76.8	50.0	73.4
Combined	0.824		98.2	75.0	95.3
Well-moderate versus poorly differentiated					
MD	0.767	0.84	76.5	82.1	80.4
Stages I and II versus III and IV					
MD	0.72	0.78	82.9	60.0	76.8

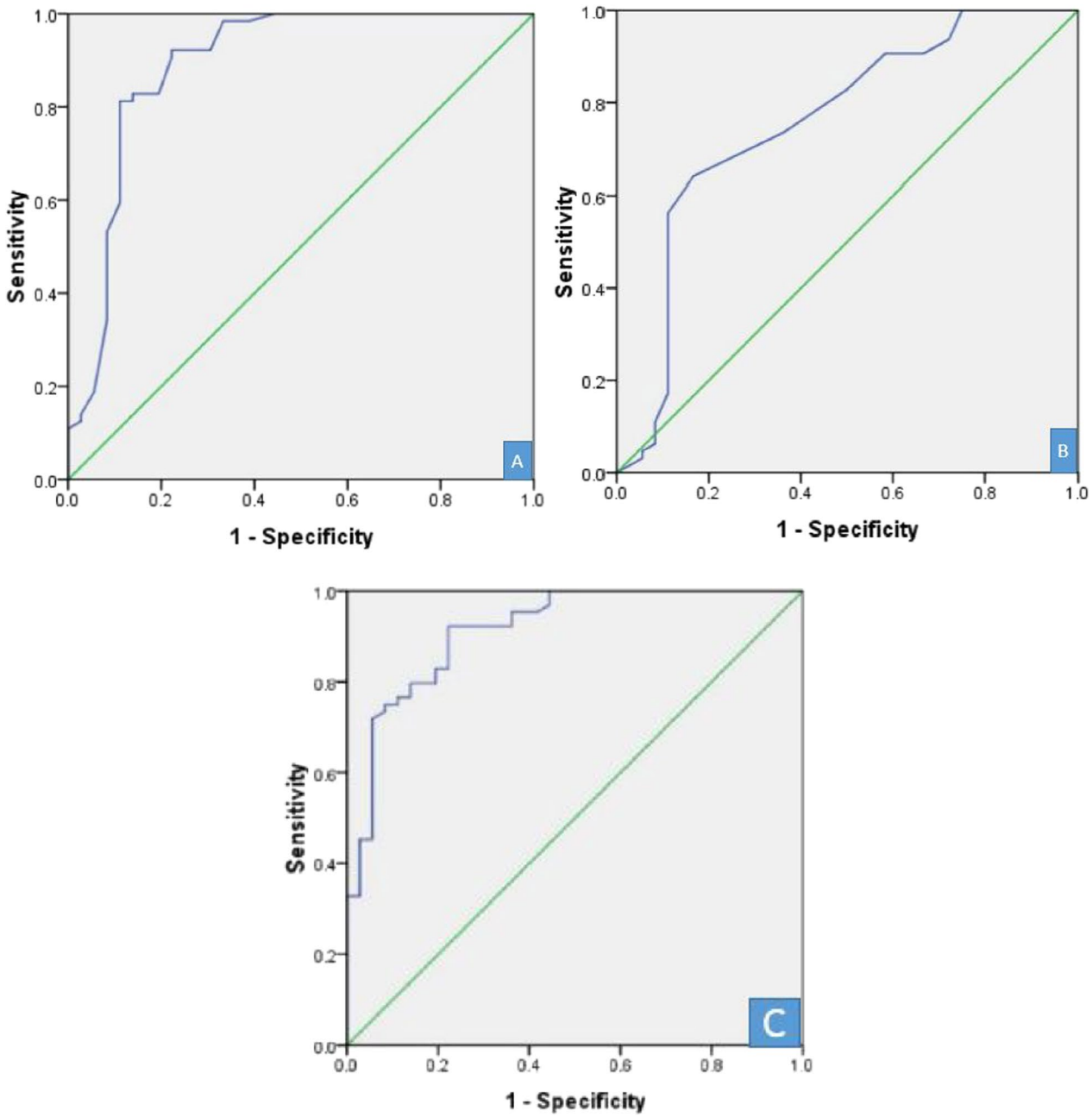

Fig. 2 ROC curve of MD and FA of malignant versus benign LNs. **A** The cutoff value of MD utilized to distinguish malignant from benign LNs is 0.94×10^{-3} mm^2/s with AUC of 0.892, an accuracy of 84%, specificity of 88.9%, and sensitivity of 81.2%. **B** The cutoff value of FA applied to distinguish malignant from benign LNs is 0.21 with an AUC 0.758, an accuracy 71%, specificity 50%, and sensitivity 82.8%. **C** Combined parameters show AUC 0.914, with an accuracy 81%, specificity 77.8%, and sensitivity 92.2%

The mean MD of well-moderately differentiated metastatic LNs ($n=39$) ($0.81\pm0.06\times10^{-3}$ mm^2/s) was statistically less than ($P=0.001$) the poorly differentiated metastatic LNs ($n=17$), ($0.96\pm0.16\times10^{-3}$ mm^2/s). The mean FA of well-moderately differentiated (0.26 ± 0.08) was higher than ($P=0.23$) that of poorly differentiated metastatic LNs (0.23 ± 0.04) but did not reach a significant value ($P=0.23$). On ROC curve analysis, the AUC of MD utilized to distinguish well-moderately from poorly differentiated metastatic LNs was 0.767 with cut-off point 0.84×10^{-3} mm^2/s, an accuracy 80.4%, sensitivity 76.5%, and specificity 82.1% (Fig. 4).

The mean of MD of metastatic LNs with stages I and II ($n=15$) [$0.88\pm0.13\times10^{-3}$ mm^2/s] was more

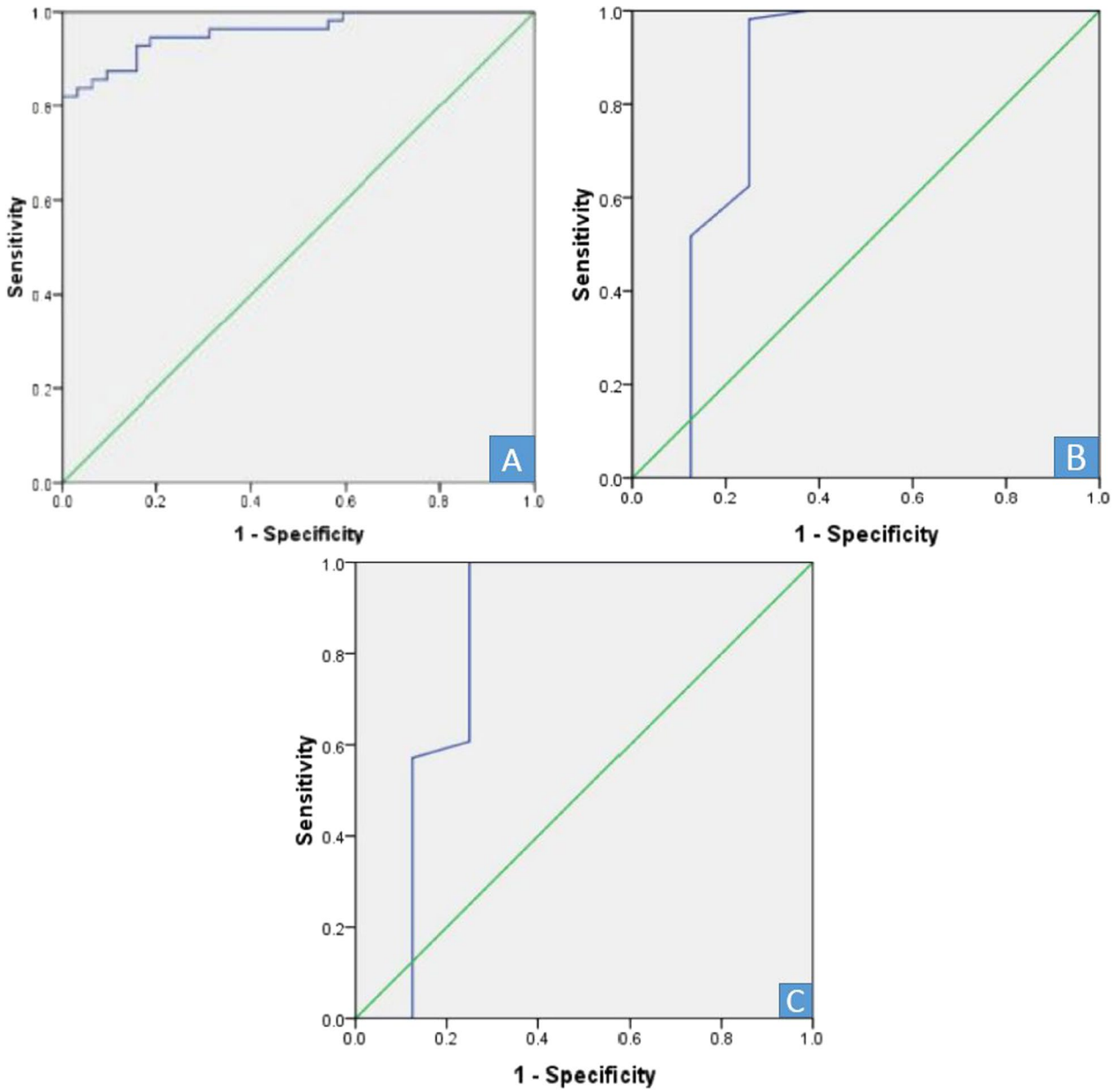

Fig. 3 ROC curve of MD and FA of metastatic versus lymphomatous LNs. **A** The cutoff value of MD applied to distinguish metastatic LNs from lymphomatous LNs is 0.71×10^{-3} mm^2/s with AUC 0.820, an accuracy 95.3%, sensitivity 98%, and specificity 75%. **B** The cutoff value of FA applied to distinguish metastatic from lymphomatous LNs is 0.27 with AUC 0.711, accuracy 73.4%, sensitivity 76.8%, and specificity 50%. **C** Combined parameters show AUC of 0.824, with accuracy 95.3%, sensitivity 98.2%, and specificity 75%

($P = 0.018$) than LNs of stages III and IV malignancy ($n = 41$) [$0.80 \pm 0.05 \times 10^{-3}$ mm^2/s]. The mean FA of metastatic LNs with stages I and II (0.22 ± 0.04) was lower than the metastatic LNs with stages III and IV (0.26 ± 0.08) but not reach to a significant level ($P = 0.69$). The AUC of MD utilized to distinguish metastatic LNs of stages I, II and stages III, IV was 0.72 with a cutoff point 0.78×10^{-3} mm^2/s, an accuracy 76.8%, sensitivity 82.9%, and specificity 60% (Fig. 5).

Discussion

The major parameters in this research were MD, and FA were used for characterization of cervical LNs. Malignant cervical LNs had restricted diffusion with higher FA,

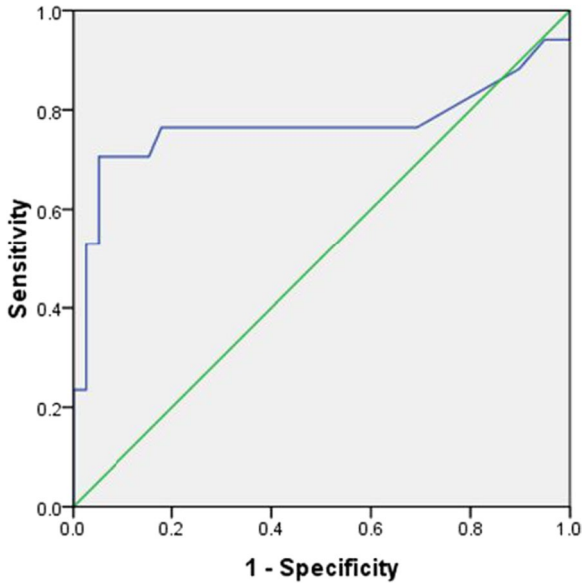

Fig. 4 ROC curve of MD for the degree of differentiation of metastatic LNs. The cutoff value of MD applied to categorize well-moderate from poorly differentiated metastatic LNs is 0.84×10^{-3} mm^2/s, AUC 0.767, accuracy 80.4%, sensitivity 76.5%, and specificity 82.1%

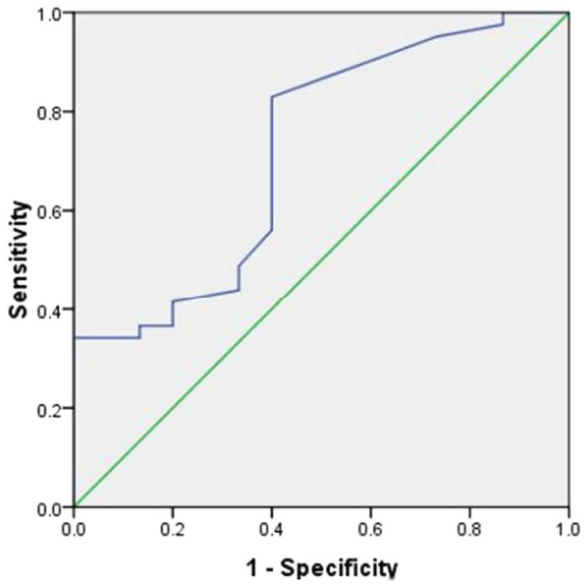

Fig. 5 ROC curve of MD for the staging of metastatic LNs. The cutoff value of MD 0.78×10^{-3} mm^2/s used to differentiate metastatic LNs of stages I, II and stages III, IV with AUC 0.72, accuracy 76.8%, sensitivity 82.9%, and specificity 60%

and benign LNs had unrestricted diffusion with lower FA. Metastatic cervical LNs revealed a higher MD and lower FA compared to lymphomatous nodes, and there was a significant statistical difference between MD of well-moderately differentiated versus poorly differentiated metastatic nodes and between metastatic nodes with stages I and II versus stages III and IV.

Malignant cervical LNs showed decreased MD compared with reactive cervical LNs, likely because of the more free water motion in reactive and the more cellularity in malignant LNs. As diffusion within malignant cervical LNs is blocked by the cellular membranes and macromolecular structures, benign LNs show limited cell mitosis rendering reduced cell concentration that would be evaluated as an elevation in the MD parameter for the enlarged LN [9–11, 23]. Previous studies concluded that MD for malignant tumors is less than those for benign lesions [35–40]. Another research found that qualitative DWI together with the conventional images allowed diagnosis of malignant LNs with sensitivity 94% and specificity 100% [38].

In this study, FA of malignant LNs was remarkably higher than benign cervical LNs. This may be attributed to that malignant LNs have high cellularity, which may lead the water molecules to flow and diffuse with a higher degree of directionality, in the contrary to non-neoplastic cervical LNs. One recent study stated that there was a significant statistical variation in FA of oral cancer compared to the normal tissue and between metastatic and non-metastatic cervical LNs [34]. Another research added that recurrent neck and head malignancy shows a more FA than post-treatment changes [38]. The combination of MD and FA of the LNs revealed the highest accuracy in distinguishing benign from malignant LNs. A recent study reported that combined MD and FA help in the definition of parotid neoplasms and differentiation of parotid malignancy from benign tumors [40].

In this research, there was a significant statistical variation in MD and FA between metastatic and lymphomatous LNs with lower MD and more FA of lymphomatous than metastatic LNs, and combination of FA and MD increased accuracy for distinguishing metastatic from lymphomatous nodes. The previous studies reported that lymphomatous nodes showed lower MD as lymphoma has greater cellularity, much larger nuclei and also, and little extra-cellular space compared to metastatic nodes [41–43].

In this study, there was a significant variation in MD between well-moderately versus poorly differentiated and lower versus high stages of metastatic LNs; however, the FA showed an insignificant difference. The degree of differentiation and staging of cervical LNs in patients with head and cervical malignancy are important for treatment planning and prognosis with a bad prognosis of poorly differentiated and higher stage of metastatic LNs [2–5]. The previous studies reported significant statistical variation in MD of the different stages and grading of

cervical LNs due to increased cellularity and fewer spaces within metastatic LNs with a higher stage and less degree of differentiation [26–30]. One recent study stated that there was a significant inverse correlation of FA with histological grades of metastatic cervical LNs [34].

There were a number of limitations to this study. Firstly, the patients' population was a small collection of LNs with different pathologies. Future multi-center study with a larger group of patients who study DTI of certain pathology would make results more appropriate. Second, the study only used DTI metrics, future studies discussing multi-parametric imaging together with dynamic susceptibility perfusion-weighted MR imaging [44–46], arterial spin labeling [47–49], and MR spectroscopy [50] with an application of artificial intelligence and deep learning [51, 52] will improve the accuracy of MR imaging in the characterization of cervical LNs.

Conclusions

Combination of MD and FA is useful non-invasive imaging parameters which could be helpful in characterization of metastatic, lymphomatous, and benign LNs, and MD has a role in grading and staging of metastatic cervical LNs.

Abbreviations

AUC	The area under curve
CT	Computed tomography
DTI	Diffusion tensor imaging
DWI	Diffusion-weighted imaging
FA	Fractional anisotropy
LNs	Lymphadenopathy/lymph nodes
MR	Magnetic resonance
MD	Mean diffusivity
ROC	Receptor operating characteristic
ROI	Region of interest
SD	Standard deviation

Acknowledgements

Not applicable.

Author contributions

Each author has participated sufficiently in this work. All authors have read and approved the manuscript.

Funding

This research did not receive any specific grant from funding agencies in the public, commercial, or not-for-profit sectors.

Availability of data and materials

On reasonable request.

Declarations

Ethics approval and consent to participate

Institutional research board approval was obtained, and informed consent from the patients was waived because this is a retrospective study.

Consent for publication

Not applicable.

Competing interests

The authors declare that they have no competing interests.

Received: 8 May 2023 Accepted: 21 July 2023
Published online: 01 August 2023

References

1. Aulino JM, Kirsch CFE, Burns J et al (2019) ACR appropriateness criteria neck mass-adenopathy. J Am Coll Radiol 16:S150–S160
2. Tanaka H (2020) Diagnostic imaging of metastatic nodal disease. In: Ojiri H (ed) Diagnostic imaging in head and neck cancer. Srpinger, Berlin, pp 113–129
3. Heřman J, Sedláčková Z, Fürst T, Vachutka J, Salzman R, Vomáčka J, Heřman M (2019) The role of ultrasound and shear-wave elastography in evaluation of cervical lymph nodes. Biomed Res Int. https://doi.org/10.1155/2019/4318251
4. Wagner JM, Alleman AM (2019) Ultrasonography of cervical lymph nodes. Radiol Clin N Am 57:485–500
5. Chung MS, Choi YJ, Kim SO et al (2019) A scoring system for prediction of cervical lymph node metastasis in patients with head and neck squamous cell carcinoma. AJNR Am J Neuroradiol 40:1049–1054
6. Hiyama T, Kuno H, Nagaki T et al (2020) Extra-nodal extension in head and neck cancer: how radiologists can help staging and treatment planning. Jpn J Radiol 38:489–506
7. Abdel Razek AA, Gaballa G (2011) Role of perfusion magnetic resonance imaging in cervical lymphadenopathy. J Comput Assist Tomogr 35:21–25
8. Treutlein C, Stollberg A, Scherl C et al (2020) Diagnostic value of 3D dynamic contrast-enhanced magnetic resonance imaging in lymph node metastases of head and neck tumors: a correlation study with histology. Acta Radiol Open 9:2058460120951966
9. Razek AAKA, Helmy E (2020) Multi-parametric arterial spin labeling and diffusion-weighted imaging in differentiation of metastatic from reactive lymph nodes in head and neck squamous cell carcinoma. Eur Arch Otorhinolaryngol. https://doi.org/10.1007/s00405-020-06390-0
10. Abdel Razek AAK (2020) Editorial for "Preliminary assessment of intravoxel incoherent motion diffusion-weighted MRI (IVIM-DWI) metrics in Alzheimer's disease." J Magn Reson Imaging 52:1827–1828
11. Abdel Razek AA, Poptani H (2013) MR spectroscopy of head and neck cancer. Eur J Radiol 82:982–989
12. Razek AA, Tawfik A, Elsorogy L et al (2014) Perfusion CT of head and neck cancer. Eur J Radiol 38:537–544
13. Tawfik AM, Razek AA, Kerl JM et al (2014) Comparison of dual-energy CT-derived iodine content and iodine overlay of normal, inflammatory and metastatic squamous cell carcinoma cervical lymph nodes. Eur Radiol 24:574–580
14. Borhani AA, Monaco SE (2017) Chapter 7 image-guided fine-needle aspiration and core needle biopsy of neck lymph nodes techniques, pearls, and pitfalls. Semin Ultrasound CT MR 38:531–541
15. Razek AA, Megahed AS, Denewer A et al (2008) Role of diffusion-weighted magnetic resonance imaging in differentiation between the viable and necrotic parts of head and neck tumors. Acta Radiol 49:364–370
16. Thoeny HC, De Keyzer F, King AD (2012) Diffusion-weighted MR imaging in the head and neck. Radiology 263:19–32
17. Abdel Razek AA, Kamal E (2013) Nasopharyngeal carcinoma: correlation of apparent diffusion coefficient value with prognostic parameters. Radiol Med 118:534–539
18. Abdel Razek A, Mossad A, Ghonim M (2011) Role of diffusion-weighted MR imaging in assessing malignant versus benign skull-base lesions. Radiol Med 116:125–132
19. Payabvash S (2018) Quantitative diffusion magnetic resonance imaging in head and neck tumors. Quant Imaging Med Surg 8:1052–1065
20. Abdel Razek A, Elkhamary S, Al-Mesfer S et al (2012) Correlation of apparent diffusion coefficient at 3 tesla with prognostic parameters of retinoblastoma. Am J Neuroradiol 33:944–948
21. Razek AA, Lattif MA, Denewer A et al (2016) Assessment of axillary lymph nodes in patients with breast cancer with diffusion-weighted MR

imaging in combination with routine and dynamic contrast MR imaging. Breast Cancer 23:525–532
22. Abdel Razek AA, Elkammary S, Elmorsy AS et al (2011) Characterization of mediastinal lymphadenopathy with diffusion-weighted imaging. Magn Reson Imaging 29:167–172
23. Zhang A, Song J, Ma Z et al (2020) Application of apparent diffusion coefficient values derived from diffusion-weighted imaging for assessing different sized metastatic lymph nodes in cervical cancers. Acta Radiol 61:848–855
24. Abdel Razek AA, Gaballa G, Elashry R et al (2015) Diffusion-weighted MR imaging of mediastinal lymphadenopathy in children. Jpn J Radiol 33:449–454
25. Razek AA, Fathy A, Gawad TA (2011) Correlation of apparent diffusion coefficient value with prognostic parameters of lung cancer. J Comput Assist Tomogr 35:248–252
26. Suh CH, Choi YJ, Baek JH et al (2018) The diagnostic value of diffusion-weighted imaging in differentiating metastatic lymph nodes of head and neck squamous cell carcinoma: a systematic review and meta-analysis. AJNR Am J Neuroradiol 39:1889–1895
27. Abdel Razek AA, Soliman NY, Elkhamary S et al (2006) Role of diffusion-weighted MR imaging in cervical lymphadenopathy. Eur Radiol 16:1468–1477
28. Payabvash S, Brackett A, Forghani R et al (2019) Differentiation of lymphomatous, metastatic, and non-malignant lymphadenopathy in the neck with quantitative diffusion-weighted imaging: systematic review and meta-analysis. Neuroradiology 61:897–910
29. Jović A, Fila J, Gršić K et al (2020) Diffusion-weighted MRI: impact of the size of the ROI in detecting metastases in subcentimeter lymph nodes in head and neck squamous cell carcinoma. Neuroradiology 62:987–994
30. Liang L, Luo X, Lian Z et al (2017) Lymph node metastasis in head and neck squamous carcinoma: efficacy of intravoxel incoherent motion magnetic resonance imaging for the differential diagnosis. Eur J Radiol 90:159–165
31. Razek AAKA, Taman SE, El Regal ME et al (2020) Diffusion tensor imaging of microstructural changes in the gray and white matter in patients with Crigler-Najjar syndrome type I. J Comput Assist Tomogr 44:393–398
32. Razek AAKA, El-Serougy L, Abdelsalam M et al (2018) Differentiation of residual/ recurrent gliomas from postradiation necrosis with arterial spin labeling and diffusion tensor magnetic resonance imaging-derived metrics. Neuroradiology 60:169–177
33. Razek AAKA, Batouty N, Fathy W et al (2018) Diffusion tensor imaging of the optic disc in idiopathic intracranial hypertension. Neuroradiology 60:1159–1166
34. Yamada I, Yohino N, Yokokawa M et al (2020) Diffusion tensor imaging of oral carcinoma: clinical evaluation and comparison with histopathological findings. Magn Reson Imaging 77:99–108
35. Li T, Sheng L, Chunyan C et al (2017) The significance of diffusion tensor magnetic resonance imaging for patients with nasopharyngeal carcinoma and trigeminal nerve invasion. Medicine 96:e6072
36. Abdel Razek AAK (2018) Routine and advanced diffusion imaging modules of the salivary glands. Neuroimaging Clin N Am 28:245–54
37. Koontz NA, Wiggins RH 3rd (2017) Differentiation of benign and malignant head and neck lesions with diffusion tensor imaging and DWI. AJR Am J Roentgenol 208:1110–1115
38. Razek AAKA (2018) Diffusion tensor imaging in differentiation of residual head and neck squamous cell carcinoma from post-radiation changes. Magn Reson Imaging 54:84–89
39. Takumi K, Fukukura Y, Hakamada H et al (2017) Value of diffusion tensor imaging in differentiating malignant from benign parotid gland tumors. Eur J Radiol 95:249–256
40. Khalek Abdel Razek AA (2018) Characterization of salivary gland tumours with diffusion tensor imaging. Dentomaxillofac Radiol 47:20170343
41. Strassen U, Geisweid C, Hofauer B et al (2018) Sonographic differentiation between lymphatic and metastatic diseases in cervical lymphadenopathy. Laryngoscope 128:859–863
42. Vidiri A, Minosse S, Piludu F et al (2019) Cervical lymphadenopathy: can the histogram analysis of apparent diffusion coefficient help to differentiate between lymphoma and squamous cell carcinoma in patients with unknown clinical primary tumor? Radiol Med 124:19–26
43. Wang YJ, Xu XQ, Hu H et al (2018) Histogram analysis of apparent diffusion coefficient maps for the differentiation between lymphoma and metastatic lymph nodes of squamous cell carcinoma in head and neck region. Acta Radiol 59:672–680
44. Razek AA, Elsorogy LG, Soliman NY et al (2011) Dynamic susceptibility contrast perfusion MR imaging in distinguishing malignant from benign head and neck tumors: a pilot study. Eur J Radiol 77:73–79
45. Abdel Razek A, Samir S, Albair G (2016) Characterization of parotid tumors with dynamic susceptibility contrast perfusion-weighted MR imaging and diffusion-weighted MR imaging. J Comput Assist Tomogr 41:131–136
46. Abdel Razek AA, Gaballa G, Ashamalla G et al (2015) Dynamic susceptibility contrast perfusion-weighted MR imaging and diffusion-weighted MR imaging in differentiating recurrent head and neck cancer from post-radiation changes. J Comput Assist Tomogr 39:849–854
47. Abdel Razek AAK, Talaat M, El-Serougy L et al (2019) Clinical applications of arterial spin labeling in brain tumors. J Comput Assist Tomogr 43:525–532
48. Abdel Razek AAK, El-Serougy L, Abdelsalam M et al (2019) Differentiation of primary central nervous system lymphoma from glioblastoma: quantitative analysis using arterial spin labeling and diffusion tensor imaging. World Neurosurg 123:e303–e309
49. Abdel Razek AAK (2018) Arterial spin labelling and diffusion-weighted magnetic resonance imaging in differentiation of recurrent head and neck cancer from post-radiation changes. J Laryngol Otol 132:923–928
50. Razek AA, Nada N (2016) Correlation of choline/creatine and apparent diffusion coefficient values with the prognostic parameters of head and neck squamous cell carcinoma. NMR Biomed 29:483–489
51. Razek AAKA (2020) Editorial for "Preoperative MRI-based radiomic machine-learning nomogram may accurately distinguish between benign and malignant soft tissue lesions: a two-center study." J Magn Reson Imaging 52:883–884
52. Zhang Y, Yu S, Zhang L et al (2020) Radiomics based on CECT in differentiating kimura disease from lymph node metastases in head and neck: a non-invasive and reliable method. Front Oncol 10:1121

Publisher's Note